JACS
JOURNAL OF THE AMERICAN CHEMICAL SOCIETY

ARTICLE

pubs.acs.org/JACS

Copper Redox Cycling in the Prion Protein Depends Critically on Binding Mode

Lin Liu,[†,#] Dianlu Jiang,[†,#] Alex McDonald,[‡] Yuanqiang Hao,[†] Glenn L. Millhauser,[*,‡] and Feimeng Zhou[*,†]

[†]Department of Chemistry and Biochemistry, California State University, Los Angeles, Los Angeles, California 90032, United States
[‡]Department of Chemistry and Biochemistry, University of California, Santa Cruz, Santa Cruz, California 95064, United States

Supporting Information

ABSTRACT: The prion protein (PrP) takes up 4−6 equiv of copper in its extended N-terminal domain, composed of the octarepeat (OR) segment (human sequence residues 60−91) and two mononuclear binding sites (at His96 and His111; also referred to as the non-OR region). The OR segment responds to specific copper concentrations by transitioning from a multi-His mode at low copper levels to a single-His, amide nitrogen mode at high levels (Chattopadhyay et al. *J. Am. Chem. Soc.* **2005**, *127*, 12647−12656). The specific function of PrP in healthy tissue is unclear, but numerous reports link copper uptake to a neuroprotective role that regulates cellular stress (Stevens, et al. *PLoS Pathog.* **2009**, *5* (4), e1000390). A current working hypothesis is that the high occupancy binding mode quenches copper's inherent redox cycling, thus, protecting against the production of reactive oxygen species from unregulated Fenton type reactions. Here, we directly test this hypothesis by performing detailed pH-dependent electrochemical measurements on both low and high occupancy copper binding modes. In contrast to the current belief, we find that the low occupancy mode completely quenches redox cycling, but high occupancy leads to the gentle production of hydrogen peroxide through a catalytic reduction of oxygen facilitated by the complex. These electrochemical findings are supported by independent kinetic measurements that probe for ascorbate usage and also peroxide production. Hydrogen peroxide production is also observed from a segment corresponding to the non-OR region. Collectively, these results overturn the current working hypothesis and suggest, instead, that the redox cycling of copper bound to PrP in the high occupancy mode is not quenched, but is regulated. The observed production of hydrogen peroxide suggests a mechanism that could explain PrP's putative role in cellular signaling.

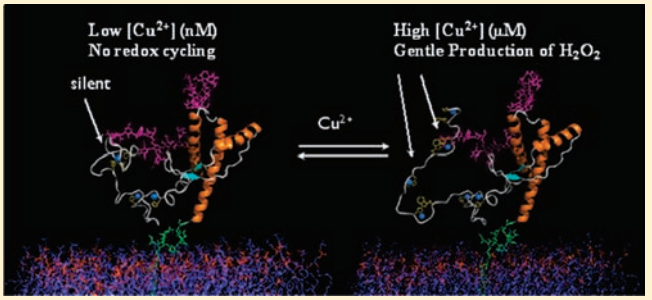

1. INTRODUCTION

The misfolding and aggregation of the prion protein (PrP), a membrane-bound glycoprotein present in the central nervous system (CNS) of mammalian and avian species, leads to the development of the prion diseases.[1,2] The human forms of prion diseases,[3] including Creutzfeldt-Jakob disease and kuru, share similar neuropathologies to other more prevalent neurodegenerative disorders such as Alzheimer's disease (AD) and Parkinson's disease (PD).[4,5] PrP has been shown to interact with a number of divalent metal ions,[6,7] and with moderate to high affinity to Cu^{2+} and Zn^{2+}.[7,8] The linkage between PrP and bioavailable Cu^{2+} is particularly well established by in vitro and in vivo[9] studies and described in a number of recent reviews.[10−14] Although copper is an essential metal and exists in a number of proteins, free Cu^{2+} exhibits high cytotoxicity, stemming from its ability to initiate redox cycling, in turn generating reactive oxygen species (ROS) via the Harber-Weiss reaction:[15−18]

$$Cu^{2+} + H_2O_2 \rightarrow Cu^{+}\cdot O_2H + H^{+} \quad (1)$$

$$Cu^{+}\cdot O_2H + H_2O_2 \rightarrow Cu^{+} + O_2 + OH\cdot + H_2O \quad (2)$$

$$H^{+} + Cu^{+} + H_2O_2 \rightarrow Cu^{2+} + OH\cdot + H_2O \quad (3)$$

The highly toxic and reactive hydroxyl radical (OH·) can readily damage DNA and proteins and cause lipid peroxidation. Reaction 3 is also referred to as a Fenton-like reaction because of its similarity to the Fenton reaction with Fe^{2+} and H_2O_2 as the reactants.[16]

In biological milieu, free or bound Cu^{2+} could initiate another redox cycle, which is dependent on the thermodynamic properties of the reactants and the structure of the Cu^{2+} complexes. The cycle starts with the reduction of free or Cu^{2+} bound to a ligand (L) by a biological reductant. The resultant Cu^{+} can be subsequently oxidized by O_2, generating H_2O_2 as a product. Using ascorbic acid (AA, which exists as ascorbate at neutral pH and oxidizes to dehydroascorbate or DA) as a representative reductant, this cycle can be described as:[19−22]

$$2L{-}Cu^{2+}\ (\text{free } Cu^{2+}) + AA + H_2O = 2L{-}Cu^{+}\ (\text{free } Cu^{+}) + DA + 2H^{+} \quad (4)$$

$$2L{-}Cu^{+}\ (\text{free } Cu^{+}) + O_2 + 2H^{+} = 2L{-}Cu^{2+}\ (\text{free } Cu^{2+}) + H_2O_2 \quad (5)$$

Received: May 17, 2011
Published: June 27, 2011

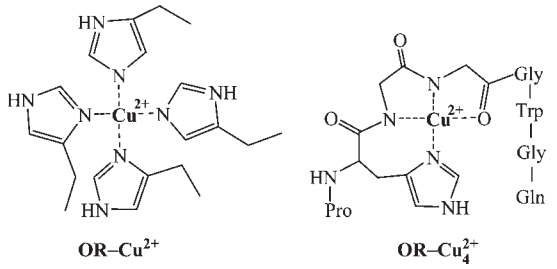

Figure 1. Structures of OR−Cu^{2+} (low Cu^{2+} occupancy) and OR−Cu_4^{2+} (high Cu^{2+} occupancy).

Notice H_2O_2 produced in reaction 5 can in turn react with any remaining free or bound Cu^{2+} through reactions 1−3 to produce OH·.

Given the abundance of oxygen[23,24] and biological reductants (e.g., AA and glutathione or GSH) in the CNS (e.g., cerebrospinal fluid (CSF) in particular), if a redox active metal were not properly regulated, the large quantity of ROS produced by the Cu^{2+}-initiated redox cycling would likely lead to significant oxidative damage. On the basis that PrP is a Cu^{2+}-binding protein,[9] a major biological function of PrP has been hypothesized to complex Cu^{2+} to attenuate or buffer its redox activity so that ROS is prevented from forming, or converted into less harmful species.[11,12] A unique feature of PrP is that distinct Cu^{2+} binding modes are populated in response to different Cu^{2+} concentrations. PrP contains a highly conserved repeat of an octapeptide (OP) sequence within its N-terminal domain that constitutes its primary sites for Cu^{2+} uptake.[11,12] Human PrP has four tandem copies of the specific sequence PHGGGWGQ (referred to as the octarepeat[11] or OR within residues 60−91). In vitro studies have shown that, when the concentration ratio between PrP and Cu^{2+} is larger than 1:1, four histidines (His) in the OR domain coordinate a single Cu^{2+} center forming the low Cu^{2+} occupancy binding mode OR−Cu^{2+} (Figure 1).[25] When the Cu^{2+} concentration rises to 4 or more equiv per protein, each of the four OPs binds one Cu^{2+}, giving rise to the so-called high occupancy or OR−Cu_4^{2+} (Figure 1).[25] In OR−Cu_4^{2+}, each Cu^{2+} is ligated by one His, the amide nitrogens on the two adjacent and deprotonated glycines, and a glycine carbonyl.[25] The OR−Cu^{2+} and OR−Cu_4^{2+} binding modes take up Cu^{2+} with highly disparate dissociation constants (0.1 nM for the former and ∼10 μM for the latter) and consequent negative cooperativity.[11,26] Immediately outside of the OR domain, the segment encompassing two His residues (in human PrP they are His96 and His111, and in mouse PrP His96 and His110) can also bind Cu^{2+}. This segment is referred to as the non-OR Cu^{2+}-binding site.[27−29] It is recently shown that, when solution pH becomes sufficiently low (∼6.0 or lower), the wild-type (WT) PrP binds a single Cu^{2+} in the OR−Cu^{2+} mode.[30] This is conceivable since His imidazoles have a lower pK_a than glycine amide nitrogens (even when they are bound to metal ions), and consequently, the Gly amide nitrogens, once protonated, are the first to lose their metal-binding ability.[11]

The multiple binding modes between Cu^{2+} and PrP and their disparate affinities have long been linked to the various functions of PrP[11,12] in modulating or inhibiting Cu^{2+} redox cycling and oxidative stress under different conditions. For example, a recent analysis of insertional mutations in the OR domain linked early onset prion disease to hindered copper uptake and decreased population of the high occupancy mode.[31] Delineation of the respective roles and/or functions of the distinct binding copper binding modes requires a clear understanding of their redox behaviors, which has been confounded by several contradictory studies. For example, Miura et al.[32] and Ruiz et al.[33] reported that the tryptophan (Trp) residues in the OR domain appear to readily reduce Cu^{2+} to Cu^{+} at both physiological and acidic pH. It was proposed that the OR−Cu^{2+} mode may allow one Trp residue to be in close vicinity to the Cu^{2+} center for a facile Cu^{2+} reduction.[32] However, many EPR studies have found that the Cu^{2+} centers bound by OR in both the low and high occupancies (even the transitory modes or stoichiometries such as OR−Cu_2^{2+} and OR−Cu_3^{2+}) are stable.[25,26,34,35] Bonomo et al. determined the redox potential of the OP−Cu^{2+} complex, which contains only one OP but has an equivalent Cu^{2+} coordination to that in OR−Cu_4^{2+}.[36] The surprisingly negative potential (∼ −0.3 V vs NHE) would silence the redox cycling of bound Cu^{2+} completely as it is lower (more negative) than those of many biological relevant reductants (e.g., AA and GSH). In other words, reaction 4 would be fully quenched. This contradicts the finding that OR−Cu_4^{2+} catalyzes the production of OH· from H_2O_2.[37] In addition, Nishikimi and co-workers[37] and Requena and co-workers[38] demonstrated that the Cu^{2+} centers in the OR domain are responsible for the oxidation of AA to DA. Owing to the above conflicting results, it has been difficult to rationalize cell-based and in vivo findings regarding the functions of PrP and its copper complexes.

A current working hypothesis, based on some of these published reports,[32,33,39] suggests that the high occupancy binding mode (OR−Cu_4^{2+}) quenches the redox cycling of free Cu^{2+}, thus, protecting against the production of ROS.[11,39] In addition, this hypothesis does not consider the detailed cellular milieu in which the catalytic cycle represented by reactions 4 and 5 might be more relevant. Such a cycle can proceed only if (I) the redox potential of L−Cu^{2+} is higher than that of the biological reductant and (II) the redox potential of L−Cu^{+} is lower than that of the O_2/H_2O_2 couple. In this work, we determined redox potentials of OR−Cu^{2+}, OR−Cu_4^{2+}, and non-OR−Cu^{2+} under an anaerobic environment and compared their voltammetric characteristics to those observed in the presence of oxygen. We demonstrate that the redox cycling observed for these complexes can be reliably predicted from redox potentials and verified by measurements of the oxidation of AA (as a common reductant) and H_2O_2 generated from the catalytic reduction of O_2. Our finding clearly shows that redox cycling of Cu^{2+} is highly dependent on the binding mode of the PrP−Cu^{2+} complexes. Moreover, contrary to the current hypothesis, we find that OR−Cu^{2+} is the binding mode that completely quenches any copper redox cycling. OR−Cu_4^{2+} leads to the gentle and controlled production of H_2O_2, which may serve as a signaling molecule to initiate various cellular events. We also examined the redox reactions of these complexes at different pH to assess how redox activity may be modulated by PrP trafficking through early and late endosomes.

2. EXPERIMENTAL SECTION

2.1. Materials. The octapeptide PHGGGWGQ (OP), an OR-containing peptide PrP(23−28, 57−91), and the PrP(91−110) peptide representing the non-OR site in mouse PrP were all prepared using solid-phase fluorenylmethoxycarbonyl (Fmoc) methods.[34,40] These peptides were acetylated at their N-termini and amidated at C-terminus. The crude products were purified by reverse-phase high-performance liquid chromatography (HPLC) and characterized by mass spectrometry. The α-synuclein (α-Syn)

Table 1. Sequences of Peptides Used in This Work

KKRPKPWGQ(PHGGGWGQ)$_4$	PrP(23−28, 57−91) or OR
PHGGGWGQ	OP
GGGTHNQWNKLSKPKTNLKH	PrP(91−110) or non-OR
DAEFRHDSGYEVHHQK	Aβ(1−16)
MDVFMKGLSKAKEGVVAAA	α-Syn(1−19)

peptide, α-Syn(1−19), was also synthesized and purified similarly. Amyloid beta (Aβ) peptide Aβ(1−16) was purchased from American Peptide Co., Inc. (Sunnyvale, CA). Table 1 lists the five peptides used in this work.

2.2. Electrochemical Measurements. Voltammetric measurements of OR−Cu^{2+}, OR−Cu_4^{2+}, and non-OR−Cu^{2+} were performed on a CHI 411 electrochemical workstation (CHI Instruments, Austin, TX) using a homemade plastic electrochemical cell. A glassy carbon disk (3 mm in diameter), a platinum wire, and a Ag/AgCl electrode served as the working, auxiliary, and reference electrodes, respectively. The electrolyte solution was a 10 mM phosphate buffer (pH 7.4) comprising 50 mM Na_2SO_4. Prior to each experiment, the glassy carbon electrode was successively polished with diamond pastes of 1 and 0.3 μm in diameter (Buehler, Lake Bluff, IL) and sonicated in deionized water. Voltammetric experiments under the oxygen-free condition were carried out in a glove box (Plas Lab, Lasing, MI) that had been thoroughly purged with and kept under N_2. The oxygen concentration in solution housed in this glove box was measured to be less than 0.05 ppm by a portable conductivity meter (Orion 3-Star Plus; Thermo Electron Corp., MA). Voltammetry was also performed in solutions purged with O_2 for a few minutes and the concentration of O_2 was maintained at ca. 8.5 ppm. To minimize free Cu^{2+} in solution and avoid its interference on the voltammograms of complexes formed between Cu^{2+} and the PrP peptides, [Cu^{2+}]/[OR] was maintained at 0.9/1 for OR−Cu^{2+} and 3.6/1 for OR−Cu_4^{2+}.

2.3. Kinetic Measurement. The AA oxidation rate was determined by monitoring the change in AA absorbance at 265 nm using a UV−vis spectrophotometer (Cary 100 Bio, Varian, Inc., Palo Alto, CA). The absorbance values plotted have excluded those contributed by the individual peptides at 265 nm (measured in separate peptide solutions of same concentrations). The kinetic experiments were conducted at 25 °C in phosphate buffer, as described by our previous studies.[22] To form exclusively OR−Cu^{2+}, it is critical to maintain the [OR]/[Cu^{2+}] ratio much higher than 1:1 so that the amount of free Cu^{2+} remaining in solution is negligible.

2.4. Detection of Hydrogen Peroxide. The H_2O_2-detection kit was purchased from Bioanalytical System, Inc. (West Lafayette, IN)[41] and the detection was conducted in a thin-layer electrochemical flow cell (Bioanalytical System, Inc.) using a hydrogel-peoxidase-modified glassy carbon electrode by following our previously published protocol.[40] Briefly, 100 μM of a given peptide was mixed with Cu^{2+} (5 μM) for 10 min. The resultant mixture was then incubated with AA (200 μM) for 2 h. The sample mixture was diluted 5-fold with phosphate buffer, prior to being injected into the electrochemical flow cell.

3. RESULTS

3.1. Redox Behavior of Cu^{2+} Complexes with PrP Peptides in Aerobic and Anaerobic Solutions. The cyclic voltammogram (CV) of OR in an oxygen-free solution reveals that it is redox inactive between −0.3 and 0.6 V versus Ag/AgCl (dotted line curve in Figure 2A). In contrast, voltammograms of OR−Cu^{2+} exhibit a redox wave with the midpoint potential ($E_{1/2}$)[42] at 0.126 V (black curve in Figure 2A). The potential value is about 0.05 V higher than that of a complex formed between a cyclic peptide (Gly-His)$_4$ and copper[43] for mimicking the putative role of superoxide dismutase-like activity of PrP.[44,45] It is also 0.06 V lower than the theoretically calculated redox potential of OR−Cu^{2+}.[46] Detailed CV studies (Figure S1 and Table S1 in the Supporting Information) indicate that the cycling between the Cu^{2+} and Cu^+ centers is quite reversible. This CV wave remains essentially unchanged when the solution is saturated with O_2 (red curve). Notice that the higher background of the CV at potential beyond −0.2 V is attributable to electrochemical reduction of dissolved O_2. Interestingly, the voltammetric behavior of OR−Cu_4^{2+} (Figure 2B) is different from that of OR−Cu^{2+} in the following aspects. First, in the absence of O_2, $E_{1/2}$ (black curve) of OR−Cu_4^{2+} was determined to be −0.025 V, a shift by 0.151 V in the negative direction with respect to that of OR−Cu^{2+}. A small shoulder wave is discernible at ca. 0.075 V, which is 0.051 V more negative than the wave of OR−Cu^{2+}. The two waves are more distinguishable in their differential pulse voltammorams (Figure S2). We assign the wave at −0.025 V to OR−Cu_4^{2+} and that at 0.051 V to the transitory binding modes in which the stoichiometry between OR and Cu^{2+} ranges between 1:2 and 1:3.[25] No Cu^0 stripping peak (vide infra) was observed, suggesting that free Cu^{2+} in the mixture is minimal. Previously, an EPR study conducted by one of us[25] has shown that OR−Cu_4^{2+} coexists with these less abundant transitory species. The second aspect is that, when O_2 is present in solution, the OR−Cu_4^{2+} CV becomes sigmoidal (i.e., the reduction peak is enhanced at the expense of the oxidation wave). Such a behavior was also observed for non-OR−Cu^{2+} (red curve in Figure 2C), albeit the latter exhibits a plateau at an even more negative potential. These sigmoidal CV waves have the same characteristics as that of free Cu^{2+} (red curve in Figure 2D), which is indicative of a catalytic process[42] in which the electrogenerated Cu^+ is rapidly reoxidized by O_2 in solution. Therefore, the Cu^+ centers in both OR−Cu_4^{2+} and non-OR−Cu^{2+} are oxidizable by O_2, a direct consequence of the negative (cathodic) shifts of their redox potentials with respect to that of OR−Cu^{2+}. In deaerated solution (Figure 2D), there is no oxygen to regenerate Cu^+ reduced from free Cu^{2+}, and consequently, Cu^+ is further reduced to Cu^0 (since Cu^+ is easier to reduce than Cu^{2+}).[42] Cu^0 deposited onto the glassy carbon electrode can then be oxidized back to Cu^{2+} during the scan reversal. The sharp anodic peak results from the stripping of the electrodeposited Cu^0.[42]

Another point worth noting is that the shift of the plateau of the red curve in Figure 2C relative to that in Figure 2B is originated from the more negative redox potential of non-OR−Cu^{2+}. In the absence of O_2 (black curve in Figure 2C), the non-OR−Cu^{2+} CV is less reversible, as evidenced by a smaller anodic peak compared to its cathodic counterpart and a wider separation in potential between the two peaks than that in the CV of OR−Cu_4^{2+} (cf. more details in Table S2).

3.2. pH-Dependent Redox Behavior of PrP−Cu^{2+} Complexes. An interesting property of PrP and its peptidic variants is that their Cu^{2+}-binding is sensitive to solution pH.[11,12,30,32] At values lower than physiological pH (e.g., ∼6.5 or lower),[30] the amide nitrogens become protonated, disfavoring the OR−Cu_4^{2+} binding mode. However, for OR−Cu^{2+}, an even lower pH is required to release the only Cu^{2+} ion, owing to the fact that Cu^{2+} is strongly coordinated by the four His residues in the OR

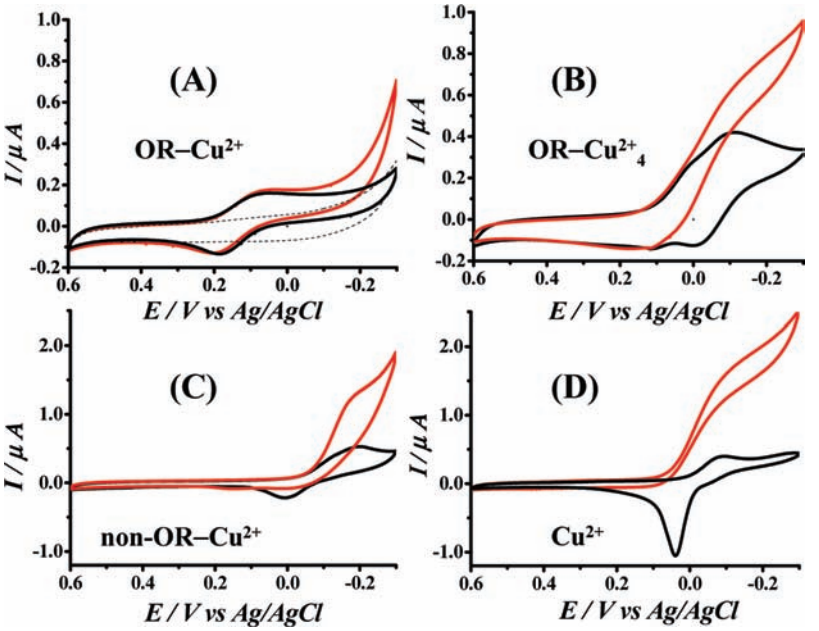

Figure 2. Cyclic voltammograms of (A) OR−Cu^{2+}, (B) OR−Cu_4^{2+}, (C) non-OR−Cu^{2+}, and (D) free Cu^{2+} in N_2-saturated (black curve) and O_2-purged solutions (red curve), respectively. The Cu^{2+} concentration in all cases was 90 μM, while the OR and non-OR concentrations were 100, 25, and 100 μM in panels (A), (B), and (C), respectively. The dotted line curve in (A) corresponds to the CV of OR. The scan rate was 5 mV/s.

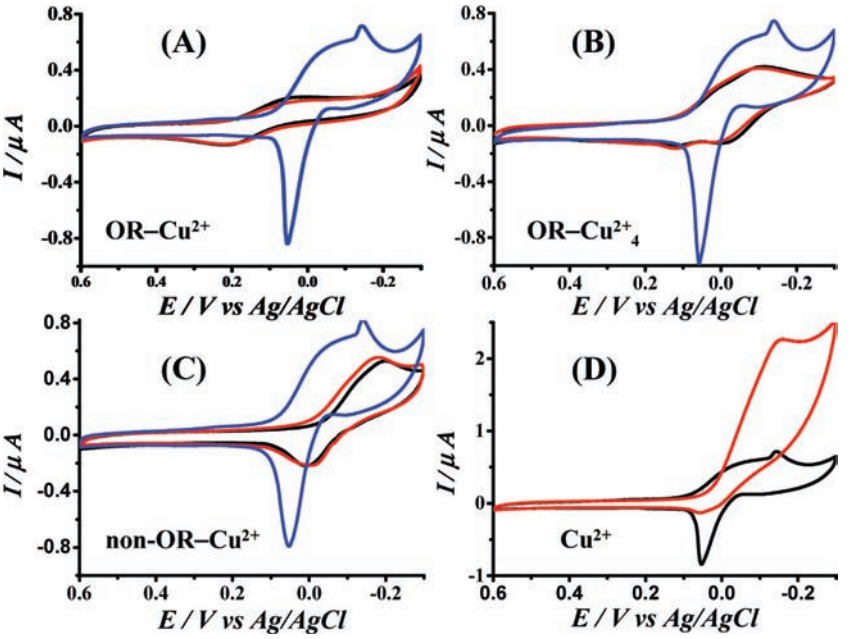

Figure 3. Cyclic voltammograms of (A) OR−Cu^{2+}, (B) OR−Cu_4^{2+}, and (C) non-OR−Cu^{2+} at different pH values. In panel (A) the curves correspond to pH 7.4 (black), 6.5 (red) and 6.0 (blue) and in panels (B) and (C) the curves correspond to 7.4 (black), 7.0 (red) and 6.0 (blue). The concentrations of Cu^{2+} and peptides used are the same as those in Figure 2. Panel (D) contrasts the voltammograms of OR−Cu^{2+} at pH 5.5 in the presence (red curve) and absence (black curve) of O_2.

domain (cf. Figure 1). We therefore examined the voltammetric responses of OR−Cu^{2+}, OR−Cu_4^{2+}, and non-OR−Cu^{2+} at different pH values and also studied the effects of O_2. Panels A and B in Figure 3 are overlaid voltammograms of OR−Cu^{2+} and OR−Cu_4^{2+} in deaerated solutions at representative pH values, respectively. As can be seen, CVs of OR−Cu^{2+} are essentially congruent between pH 7.4 and 6.5 and only until pH 6.0 does the CV begin to show a drastic change. At pH 6.0 and lower, the CV is analogous to that of free Cu^{2+} under anaerobic condition (cf. the black curve in Figure 2D) and peaks associated with OR−Cu^{2+} are no longer observable. For OR−Cu_4^{2+}, the Cu^{2+} release occurs at a higher pH (6.5), consistent with the above-mentioned fact that protonation of the Gly amide nitrogens destabilizes the OR−Cu_4^{2+} complex. A close examination of the CVs collected at pH 7.4 (black curve) and 7.0 (red curve) reveals that even with such a small pH variation,

Table 2. Redox Potentials of Cu^{2+} Complexes with Select Amyloidogenic Molecules and Biological Redox Couples

species	$E_{1/2}$ or E^0 vs Ag/AgCl (V)	vs NHE (V)	references
OR−Cu^{2+}/ OR−Cu^{+}	0.126 V	0.323 V	This work
O_2/H_2O_2	0.099	0.296	48
Aβ−Cu^{2+}/Aβ−Cu^{+}	0.080	0.277	47
PrP−Cu_S^{2+}/PrP−Cu_S^{+}	0.070	0.267	30
α-Syn−Cu^{2+}/α-Syn−Cu^{+}	0.018	0.215	40
OR−Cu_4^{2+}/ OR−Cu_4^{+}	−0.025	0.172	This work
Free Cu^{2+}/Cu^{+}	−0.040	0.157	42
non-OR−Cu^{2+}/non-OR−Cu^{+}	−0.087[a]	0.110[a]	This work
AA/DA	−0.145	0.052	49
GSH/GSSG	−0.425	−0.228	50

[a] Accuracy is affected by the less reversible redox wave of non-OR−Cu^{2+}.[42]

some Cu^{2+} release appears to have taken place. This is reflected by the small increase of the wave at around 0.051 V (red curve), which is given rise by the transitory species such as OR−Cu_2^{2+} and/or OR−Cu_3^{2+}. As mentioned above, these species are better resolved in their differential pulse voltammograms (Figure S2). Thus, as soon as some Cu^{2+} ions are released from OR−Cu_4^{2+}, OR might have rearranged to bind the remaining Cu^{2+} ions with the available His residue(s). As for non-OR−Cu^{2+}, a 0.4-unit pH decrease causes the redox wave to shift by 0.01 V in the anodic direction (cf. the red and black curves in Figure 3C).

To verify that in aerated solution Cu^{2+} released from the complexes behaves the same as free Cu^{2+} in ligand-free solutions, we also collected CVs of the three complexes at lower pH values. Figure 3D compares the CVs of OR−Cu^{2+} in deaerated (black) and aerated (red) solutions at pH 5.5. The trend is essentially the same as that of free Cu^{2+} (cf. Figure 2D). OR−Cu_4^{2+} or non-OR−Cu^{2+} also displayed very similar behaviors at higher pH (data not show). Thus, Cu^{2+} ions, once released from these complexes, are capable of initiating redox cycles. The relevance of our data to the hypothesis that PrP acts as a Cu^{2+} transporter via endocytosis is described in the Discussion section.

3.3. Relationship between the Cu^{2+} Binding Mode and the H_2O_2 Production. Through voltammetric studies of Cu^{2+} complexes with amyloid β (Aβ) peptides,[47] which are linked to the neuropathology of AD, and α-synuclein (α-syn),[40] which is believed to lead to the development of PD, we have demonstrated that H_2O_2 is indeed a product generated through reactions 4 and 5.[40,47] Therefore, we are interested in probing whether H_2O_2 can be generated by one or more of the PrP−Cu^{2+} complexes. In Table 2, we contrast the redox potentials of OR−Cu^{2+}, OR−Cu_4^{2+}, and non-OR−Cu^{2+} to those of the O_2/H_2O_2 and AA/DA couples. It is evident that, from the thermodynamic viewpoint, O_2 is incapable of oxidizing OR−Cu^{+}. In other words, the single Cu^{+} center is so "stabilized" by OR that O_2 cannot turn it over to Cu^{2+} (i.e., reaction 5 would not occur). In contrast, both the OR−Cu_4^{2+} (high occupancy) and non-OR−Cu^{2+} modes have lower redox potentials than the O_2/H_2O_2 couple and therefore are expected to behave similarly to the Cu^{2+} complexes of Aβ and α-syn to facilitate the catalytic O_2 reduction.

The above thermodynamic prediction was verified by two experiments. First, we determined the kinetics of AA oxidation by O_2 in the presence of OR−Cu^{2+}, OR−Cu_4^{2+}, or non-OR−Cu^{2+} by monitoring the change of AA absorbance at 265 nm. As shown by the green curve in Figure 4A, the rate of AA autoxidation was found to be exceedingly slow (0.051 ± 0.004 nM s^{-1}). The rate did not change with the addition of 5 μM OR−Cu^{2+} (0.048 ± 0.004 nM s^{-1}), but AA becomes rapidly consumed when the same amount of OR−Cu_4^{2+} (42.2 ± 4.7 nM s^{-1}), non-OR−Cu^{2+} (34.8 ± 3.7 nM s^{-1}), or free Cu^{2+} (191 ± 17.2 nM s^{-1}) is present. However, AA can be instantaneously and significantly oxidized by OR−Cu^{2+} at a concentration stoichiometrically more comparable to that of AA. Notice that the absorbance of a 200 μM AA solution decreased by ∼28% immediately upon being mixed with 100 μM OR−Cu^{2+} (magenta curve). The oxidation of AA is quantitative, since such a decrease is close to the theoretical value (∼25%). This observation is also confirmed by a separate differential pulse voltammetric experiment (Figure S3). Thus, the inability of O_2 to oxidize OR−Cu^{+} results in a halt of the Cu^{2+} redox cycling, preventing additional AA from being continuously oxidized. In the second experiment, we demonstrated that (1) H_2O_2 is indeed a product of the redox cycle and (2) the amount of H_2O_2 produced can be correlated to the redox potential of the Cu^{2+} complexes with select peptides. Specifically, using a commercial electrochemical H_2O_2 detection kit,[40] we found that after 2 h of reaction the amount of H_2O_2 generated in the presence of OR−Cu^{2+} is essentially negligible, whereas H_2O_2 was detected in the presence of other species. The amount of H_2O_2 increases in the order of Aβ(1−16)−Cu^{2+} < α-syn-(1−19)−Cu^{2+} < non-OR−Cu^{2+} < OR−Cu_4^{2+} (Figure 4B), which is largely consistent with the order of the redox potentials of the respective complexes (Table 2). It is worth noting that we chose the Cu^{2+}-binding peptidic segments of the full-length Aβ peptide and the α-syn protein, because the resultant complexes are more comparable to OR−Cu^{2+} or OR−Cu_4^{2+} in terms of their sizes and O_2 accessibility to the copper center.[47]

3.4. Time and pH Dependences of the H_2O_2 Production. At different solution pH, we also monitored the production of H_2O_2 as a function of time. Again, OR−Cu^{2+} generates little H_2O_2 (even over a period of 2 h as shown by Figure 5A). In contrast, H_2O_2 generated by OR−Cu_4^{2+} or non-OR−Cu^{2+} increases gradually with time. However, the amounts of H_2O_2 produced by these complexes are substantially lower than that by free Cu^{2+}, especially at the beginning of the redox cycle (magenta curve in Figure 5A). We also measured the amount of H_2O_2 generated by the Cu^{2+}-glutamine complex, on the basis that glutamine is the most abundant amino acid in CSF (more than 10 times higher than other amino acids and also albumin, a major Cu^{2+}-transport protein[24]). Using $10^{12.5}$ for the formation constant of the Cu-$(Gln)_2$ complex[51] and adjusted to pH 7.0, the $Cu(Gln)_2$ complex has an affinity constant of 0.32 μM, which is between those of OR−Cu^{2+} (0.1 nM) and OR−Cu_4^{2+} (7.0−12.0 μM).[26] That much more H_2O_2 was generated by the $Cu(Gln)_2$ complex (see the green curve in Figure 5A) suggests that, in addition to the binding affinity, other structural factors (e.g., accessibility to the Cu^{2+} center(s) by cellular reductants and O_2) are also important. Thus, OR−Cu^{2+} completely quenches the Cu^{2+} redox cycling, while OR−Cu_4^{2+} and non-OR−Cu^{2+} are capable of reducing the amount of H_2O_2 production.

The initial sharp rises of the blue and green curves in Figure 5A can be attributed to the rapid production of H_2O_2 via reactions 4 and 5 by free Cu^{2+} or the glutamine-Cu^{2+} complex. The more gradual decay is a convoluted result of the continuous H_2O_2 production via this redox cycle and the decomposition of H_2O_2 by free Cu^{2+} or the glutamine-Cu^{2+} (Glu−Cu^{2+}) complex via reactions 1−3. Thus, as H_2O_2 builds up in the solution, reactions 1−3 will accelerate to decrease the amount of H_2O_2. However, in

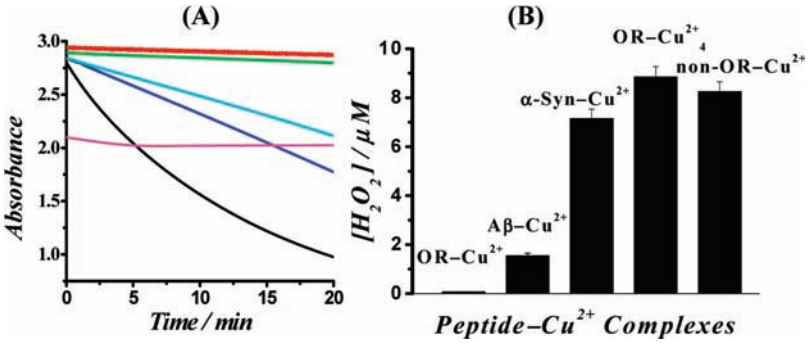

Figure 4. (A) Change of AA (200 μM) absorbance as a function of reaction time in the absence (green curve) and presence of different Cu^{2+}-containing species: OR$-Cu^{2+}$ (red curve), non-OR$-Cu^{2+}$ (cyan), OR$-Cu_4^{2+}$ (blue), and free Cu^{2+} (black). The magenta curve corresponds to the AA absorbance variation recorded after the addition of 100 μM OR$-Cu^{2+}$ to 200 μM AA solution. (B) Amounts of H_2O_2 generated by OR$-Cu^{2+}$, Aβ(1$-$16)$-Cu^{2+}$, α-syn(1$-$19)$-Cu^{2+}$, OR$-Cu_4^{2+}$, and non-OR$-Cu^{2+}$. [Cu^{2+}] was 5 μM, and concentrations of the peptide molecules were all 100 μM except for the solution of OR$-Cu_4^{2+}$ wherein [OR] = 1.25 μM.

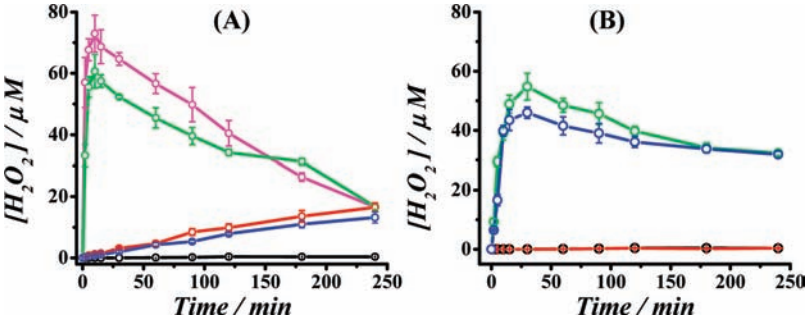

Figure 5. (A) Time-dependence of H_2O_2 generation in different solutions: OR$-Cu^{2+}$ (black), OR$-Cu_4^{2+}$ (red), non-OR$-Cu^{2+}$ (blue), Cu^{2+}–glutamine (green), and free Cu^{2+} (magenta). All solutions contained 5 μM Cu^{2+} and 200 μM AA and the ligand concentration was 100 μM except for the solution of OR$-Cu_4^{2+}$ wherein [OR] = 1.25 μM. (B) Variations of [H_2O_2] generated by OR$-Cu^{2+}$ in solutions of different pH values: 7.4 (black), 6.5 (red), 6.0 (green), and 5.5 (blue). Each data point is the average of three replicates and the error bars are the standard deviations.

this case, the more reactive and pernicious hydroxyl radicals are formed. The biological implication of the H_2O_2 generation as well as the complete inhibition of the H_2O_2 and hydroxyl radical productions by these Cu^{2+} complexes will be presented in the Discussion.

Finally, we determined the time dependence of H_2O_2 production by the Cu^{2+} complexes at different solution pH. Figure 5B displays representative results measured and plotted for OR$-Cu^{2+}$ at pH 7.4, 6.5, 6.0, and 5.5. When Cu^{2+} is bound, no (for OR$-Cu^{2+}$) or a small amount of H_2O_2 (for OR$-Cu_4^{2+}$ and non-OR$-Cu^{2+}$; data not shown) was produced. However, as the solution pH is lowered, all complexes exhibit the same trend as depicted by the green and blue curves in Figure 5B, suggesting that Cu^{2+} released from these complexes becomes predominant in producing H_2O_2 and possibly hydroxyl radicals. Thus, at physiological pH, all the binding domains possess the ability of preventing a large amount of H_2O_2 from being produced and completely annihilating the possibility of hydroxyl radical generation. This aspect will be reiterated below in connection with the discussion of the possible functions of PrP.

4. DISCUSSION

Using carefully controlled anaerobic and aerated solutions, we conducted a systematic investigation on the electrochemical behaviors of OR$-Cu^{2+}$, OR$-Cu_4^{2+}$, and non-OR$-Cu^{2+}$. Comparison of the respective redox potentials of these complexes to those of the O_2/H_2O_2 and AA/DA couples (cf. Table 2) clearly indicates that, thermodynamically, the Cu^{2+} centers in these complexes can all be reduced by common cellular reductants (e.g., AA and GSH). However, the occurrence of the Cu^{2+} redox cycle described by reactions 4 and 5 to generate H_2O_2 also requires the Cu^{+} centers be oxidizable by O_2. On the basis of the shifts in the reduction potentials of the complexes with respect to that of free Cu^{2+}, we determined that, in the OR$-$copper complex (low occupancy), binding of Cu^{+} by OR is about 3 orders of magnitude stronger than that of Cu^{2+} (Supporting Information). Thus, by significantly shifting the redox potential of the bound Cu^{2+} in the anodic direction, the low occupancy binding mode completely inhibits the H_2O_2 generation. In contrast, binding affinities of Cu^{2+} and Cu^{+} in the high occupancy mode are comparable. We found that non-OR binds Cu^{+} about 4.7 times less strongly than Cu^{2+} (Supporting Information). As a consequence, non-OR$-Cu^{2+}$ can also facilitate the H_2O_2 generation. The reported redox potentials of complexes of shorter non-OR peptides with copper are 0.24 V for the GGGTH$-Cu^{2+}$ complex[29] and 0.32 V for the GGGTHSQW$-Cu^{2+}$ complex,[52] both of which are much higher than 0.110 V we measured for non-OR$-Cu^{2+}$. From the thermodynamic viewpoint, GGGTHSQW$-Cu^{2+}$ would not be capable of facilitating the redox cycling of Cu^{2+} if its redox potential were 0.32 V. The results from both the UV$-$vis spectrophotometric measurements of AA oxidation and electrochemical quantification of H_2O_2 (Figure 4) are fully consistent with our thermodynamic reasoning. This firmly establishes a correlation between a specific Cu^{2+} binding

mode in PrP and the protein's ability to ameliorate oxidative stress. It is worth mentioning that the properties of the complexes not only depend on what and how many amino acid residues are involved in the binding, but also are governed by the environment and steric hindrance under which the residues are bound to the Cu^{2+} center. We noticed that the complex formed between $(Gly\text{-}His)_4$ and Cu^{2+} has a potential that is 0.05 V more negative than OR$-Cu^{2+}$.[43] Such a difference is expected to make this complex behave similarly to the A$\beta-Cu^{2+}$ complex (cf. Table 2), leading to the Cu^{2+} redox cycling to produce H_2O_2. It is also interesting to note that the redox potential of OR$-Cu^{2+}$ (0.323 V vs NHE; cf. Table 2) is very close to that of superoxide dismutase or SOD (0.32 V).[43] While this may be used to argue for the SOD-like behavior of the PrP$-Cu^{2+}$ complex,[44] we should point out that the reported "SOD-like activity" of PrP$-Cu^{2+}$ is at least 2 orders of magnitude smaller than that of native SOD.[45] In addition, there are other large differences in structures and properties between the PrP$-Cu^{2+}$ complex and native SOD that make the correlation of the PrP$-Cu^{2+}$ complex to SOD questionable.[11,12]

The significance of our findings is threefold. First, with a better understanding of the redox behavior of the PrP$-Cu^{2+}$ complexes, several major discrepancies in the literature may now be clarified. As mentioned in the Introduction, the current paradigm suggesting that OR$-Cu_4^{2+}$, instead of OR$-Cu^{2+}$, is the more effective binding mode for quenching Cu^{2+} redox cycling now becomes questionable.[11,12] Our new paradigm provides theoretical supports for the work of Shiraishi et al.[37] and Requena and co-workers[38] in that AA can be directly oxidized by both OR$-Cu_4^{2+}$ and OR$-Cu^{2+}$, but only the latter completely quenches the copper redox cycling. Regarding the reduction of Cu^{2+} by Trp inherent in the OR domain of PrP, we believe that the use of bathocuproine (BC) to assay the redox activity of PrP$-$copper complexes can be problematic. Despite the cautions advocated by Sayre[53] and Ivanov et al.,[54] BC and its derivatives are still widely used for studying reduction of Cu^{2+} bound by biomolecules to Cu^+. With a strong binding affinity, BC can seize Cu^{2+} from certain biomolecules and bind it in the form of $(BC)_2-Cu^{2+}$, which has a much higher oxidation potential than free Cu^{2+} and many other Cu^{2+} complexes.[53] Consequently, when oxidizable ligands are present in the system (e.g., His, Tyr, Trp, and Cys residues on protein molecules), Cu^+ is produced and bound by BC, with the simultaneous oxidation of these redox-active moieties. Another important issue is that the Cu^{2+} redox cycling (or lack of) shown by reactions 4 and 5 is not only dependent on the conversion of Cu^{2+} to Cu^+ by an endogenous reductant, but also governed by the requirement that Cu^+ remaining bound to PrP must then be oxidized back by O_2 to Cu^{2+}. Thus, to simply ascribe the absence or presence of a redox cycle to the "stabilization" of Cu^{2+} or Cu^+ might not be the most accurate interpretation on the role of PrP in inhibiting Cu^{2+}-induced ROS production. Finally, OR$-Cu^{2+}$ is also more effective in inhibiting ROS production than the A$\beta-Cu^{2+}$ and α-syn$-Cu^{2+}$ complexes. High levels of Cu^{2+} have been found to be complexed by Aβ peptides in senile plaques[55] and by α-syn in CSFs of patients.[56] Such observations have been used to suggest the pro- or antioxidation functions of these amyloidogenic species.[17,55−59]

The second outcome of our study is that the voltammetric responses of the three PrP$-Cu^{2+}$ complexes each exhibit a different dependence on solution pH. The pH sensitivity of PrP$-Cu^{2+}$ and the demonstration that high copper levels (e.g., 100 μM[60]) stimulate PrP endocytosis have been used to advance the hypothesis that PrP may function as a copper transporter. Once becoming internalized and incorporated by endosomes, Cu^{2+} could be released from the complex due to the acidic environment of the endosome.[11,32] Although this copper-transport model is still under debate[11,12] and the fate of internalized PrP or the bound and released Cu^{2+} is not known, our results suggest that PrP with Cu^{2+} bound in different modes may undergo different endocytotic processes. It is well established that pH is only slightly acidic (~6.3−6.8) in the tubular extension of the early endosome, whereas it decreases from 6.2 to ~5.5 in the lumen of multivesicular bodies.[61] The tubular extension is mainly responsible for the recycling of proteins, while the multivesicular bodies, a feature characteristic of the late endosome, are involved in sorting its cargo to the degradation pathway.[62] PrP fully loaded with Cu^{2+}, once encountering the slightly acidic environment of the early endosome, can release most of its Cu^{2+} complement. In contrast, Cu^{2+} is strongly withheld by OR in the OR$-Cu^{2+}$ mode, even at the much lower pH inside the multivesicular bodies. Indeed, Brown and colleagues recently showed that at pH 5.5 or even lower, a single Cu^{2+} remains bound to the WT PrP in the OR domain. At a higher pH (~6.0), non-OR becomes capable of binding Cu^{2+} and the incorporation of additional Cu^{2+} ions into the OR domain occurs only after the solution pH has approached to the physiological value.[30] On the basis of our pH-dependence study (Figure 3), we hypothesize that Cu^{2+} released from the fully loaded PrP, through either subsequent complexation with other copper-binding proteins or generation of H_2O_2, may trigger the accumulation of PrP in the tubular extension of the early endosome, which ultimately leads to recycling of PrP back to plasma membrane. As for PrP containing only one Cu^{2+}, it could remain bound to PrP even in the late endosome, which is eventually fused with the lysosome for the final protein and metal degradation.[62]

Finally, we note that the distinct electrochemical features associated with each binding mode may provide insight into PrP function. PrP has been suggested to serve as a neuroprotectant by scavenging weakly complexed Cu^{2+} in vivo and thereby alleviating oxidative stress that might be induced by free Cu^{2+}.[31,63] The gradual generation of H_2O_2 by either OR$-Cu_4^{2+}$ or non-OR$-Cu^{2+}$ does not contradict the proposed neuroprotecting function of PrP. As can be seen from Figure 5, the amount of H_2O_2 generated by OR$-Cu_4^{2+}$ or non-OR$-Cu^{2+}$ is much lower than those generated by free Cu^{2+} and the $Cu^{2+}-$glutamine complex (glutamine is the dominant amino acid in CSF), especially at the beginning of the redox cycle. Although H_2O_2 as a ROS could also inflict oxidative stress/damage, we note that in vivo H_2O_2 is readily decomposed by enzymes such as catalase and GSH peroxidase or reacted away with antioxidants such as AA and GSH. Therefore, a harmful buildup of H_2O_2 given rise by the PrP$-Cu^{2+}$ complexes is unlikely. It was estimated that up to 250 μM H_2O_2 could be produced within brain neuropil every minute.[64] The H_2O_2 concentration depicted in Figure 5A (sub-μM levels produced by AA at a physiologically relevant concentration at the beginning) is only a small fraction of the known endogenous H_2O_2 concentration in the CNS. Therefore, the capacity of brain homeostasis of endogenous H_2O_2 appears to be more than sufficient to reduce any adverse effects that might be caused by H_2O_2 generated by the PrP$-Cu^{2+}$ complexes. More importantly, our observation of the in vitro production of H_2O_2 is supported by the cell culture work conducted by Nishimura et al.[65] In their work, the PrP-deficient neurons were found to be more susceptible to Cu^{2+} toxicity than normal neurons. In addition, in the presence of Cu^{2+}, more intracellular H_2O_2 was detected in the media of normal neurons and the viability of these neurons is not greatly impacted. This is consistent with the common belief that H_2O_2 is much less potent than the oxygen-containing radicals (e.g., $OH^{\cdot}$) and does not readily cause oxidative damage.[66−68] In fact, Rice and co-workers did not detect lipid peroxidation in cell membranes when dopaminergic neurons were exposed to high dosage of

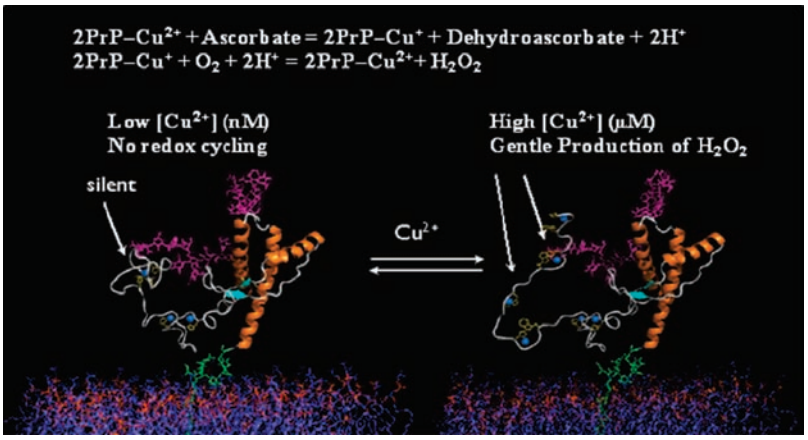

Figure 6. Schematic representation of the possible roles of PrP−Cu^{2+} complexes in quenching the Cu^{2+} redox cycling or gradual production of H_2O_2 for signal transduction. PrP is tethered to cell membrane via the glycosylphosphatidylinositol (GPI) anchor (green) with its α-helices in the C terminus shown in orange, N-linked carbohydrates in purple, and the OR and non-OR domains near the N-terminus depicted in white. When $[Cu^{2+}]$ is at a low level (nM or lower) and at pH ranging between 5.5 and 7.4, Cu^{2+} (blue sphere) remains bound in the OR−Cu^{2+} mode (left), quenching the Cu^{2+} redox cycling. At higher $[Cu^{2+}]$ (μM) and a pH closer to the physiological value, the binding mode transitions to OR−Cu_4^{2+} (right), leading to a gradual and controlled production of H_2O_2. Coordinates for the PrP C-terminal domain, along with carbohydrates, GPI anchor, and membrane, were kindly provided by Professor Valerie Daggett (U. Washington).

H_2O_2.[64] Taken together, as summarized in Figure 6, we propose that H_2O_2 generated at the PrP-residing membrane could act as an important signaling molecule. There is a growing body of evidence demonstrating that H_2O_2 is a signaling messenger capable of modulating synaptic activities and triggering a variety of cellular events.[23,67−70] Indeed, Herms et al. have reported that 0.001% exogenous H_2O_2 enhances inhibitory synaptic activity in wild-type mouse Purkinje cells.[71] More relevantly, a prominent mechanism for H_2O_2-triggered cell signaling involves diffusion of H_2O_2 from extracellular space to cytosol to enhance protein tyrosine phosphorylation via simultaneous inactivation of tyrosine phosphotases and activation of tyrosine kinases.[69] In support of this mechanism, we note that Mouillet-Richard and co-workers suggested a role for PrP in signal transduction that might be facilitated by coupling of the membrane-anchored PrP to the intracellular tyrosine kinase Fyn through an unidentified signaling molecule.[72]

In conclusion, we demonstrate that the occurrence/inhibition of the redox cycling of Cu^{2+} by PrP is dependent on binding mode. The voltammetric data, kinetic studies, and H_2O_2 detection and quantification unequivocally indicate that OR−Cu^{2+} is the most effective mode in inhibiting the Cu^{2+} redox cycling and in sequestering uncomplexed Cu^{2+}, thus, minimizing possible oxidative damage. Specifically, at nanomolar or lower Cu^{2+} concentrations, which favor the formation of OR−Cu^{2+}, the complete abolishment of redox cycling of Cu^{2+} by PrP is realized by shifting the redox potential of the resultant complex out of the range wherein the complexed Cu^{+} is oxidizable by O_2 (Figure 6). As free or weakly complexed Cu^{2+} concentration increases to micromolar levels, the binding mode transitions to high Cu^{2+} occupancy, which facilitates the redox cycling of Cu^{2+} and conversion of O_2 to H_2O_2. Such results challenge the currently held hypothesis that the high occupancy mode quenches Cu^{2+} redox cycling. We show that both OR−Cu_4^{2+} and non-OR−Cu^{2+} produce H_2O_2 in a controlled and gradual manner. Instead of producing a large amount of H_2O_2 that might inflict cellular damage, H_2O_2 generated at a lower level probably serves as a cellular signal to initiate important cellular processes. We therefore suggest that OR−Cu^{2+}, OR−Cu_4^{2+}, and non-OR−Cu^{2+} all contribute to the maintenance of neuronal integrity by inhibiting the formation of the radical forms of ROS and regulating the endocytotic processes, perhaps through an H_2O_2 dependent signaling mechanism.

■ ASSOCIATED CONTENT

Supporting Information. Additional experimental details about the electrochemical studies. This material is available free of charge via the Internet at http://pubs.acs.org.

■ AUTHOR INFORMATION

Corresponding Author
glennm@ucsc.edu; fzhou@calstatela.edu

Author Contributions
#These authors contributed equally.

■ ACKNOWLEDGMENT

Partial support of this work by the NIH (SC1MS070155-01 to F.Z. and GM065790 to G.L.M.) is gratefully acknowledged. F.Z. also acknowledges support from the NIH-RIMI Program at California State University, Los Angeles (P20-MD001824-01).

■ REFERENCES

(1) Prusiner, S. B. *Science* **1997**, *278*, 245–251.
(2) Cobb, N. J.; Surewicz, W. K. *Biochemistry* **2009**, *48*, 2574–2585.
(3) Brandner, S. *Br. Med. Bull.* **2003**, *66*, 131–139.
(4) Dawson, T. M., Ed. *Parkinson's Disease*; Informa Healthcare USA, Inc: New York, 2007.
(5) Sisodia, S. S.; Tanzi, R. E., Eds. *Alzheimer's Disease*; Springer: New York, 2007.
(6) Gaggelli, E.; Bernardi, F.; Molteni, E.; Pogni, R.; Valensin, D.; Valensin, G.; Remelli, M.; Luczkowski, M.; Kozlowski, H. *J. Am. Chem. Soc.* **2005**, *127*, 996–1006.
(7) Pandey, K. K.; Snyder, J. P.; Liotta, D. C.; Musaev, D. G. *J. Phys. Chem. B* **2010**, *114*, 1127–1135.

(8) Walter, E. D.; Stevens, D. J.; Visconte, M. P.; Millhauser, G. L. *J. Am. Chem. Soc.* **2007**, *129*, 15440–15441.
(9) Brown, D. R.; Qin, K.; Herms, J. W.; Madlung, A.; Manson, J.; Strome, R.; Fraser, P. E.; Kruck, T.; von Bohlen, A.; Schulz-Schaeff, W.; Giese, A.; Westaway, D.; Kretzschmar, H. *Nature* **1997**, *390*, 684–687.
(10) Gaggelli, E.; Kozlowski, H.; Valensin, D.; Valensin, G. *Chem. Rev.* **2006**, *106*, 1995–2044.
(11) Millhauser, G. L. *Acc. Chem. Res.* **2004**, *37*, 79–85.
(12) Millhauser, G. L. *Annu. Rev. Phys. Chem.* **2007**, *58*, 299–320.
(13) Singh, N.; Singh, A.; Das, D.; Mohan, M. L. *Antioxid. Redox Signaling* **2009**, *12*, 1271–1294.
(14) Vassallo, N.; Herms, J. *J. Neurochem.* **2003**, *86*, 538–544.
(15) Koppenol, W. H. *Redox Rep.* **2001**, *6*, 229–234.
(16) Barb, W. G.; Baxendale, J. H.; George, P.; Hargrave, K. R. *Trans. Faraday Soc.* **1951**, *47*, 462–500.
(17) Baruch-Suchodolsky, R.; Fischer, B. *Biochemistry* **2009**, *48*, 4354–4370.
(18) Halliwell, B.; Gutteridge, J. M. *Methods Enzymol.* **1990**, *186*, 1–85.
(19) Silverblatt, E.; Robinson, A. L.; King, C. G. *J. Am. Chem. Soc.* **1943**, *65*, 137–141.
(20) Srogl, J.; Voltrova, S. *Org. Lett.* **2009**, *11*, 843–845.
(21) Strizhak, P. E.; Basylchuk, A. B.; Demjanchyk, I.; Fecher, F.; Schneider, F. W.; Münster, A. F. *Phys. Chem. Chem. Phys.* **2000**, *2*, 4721–4727.
(22) Jiang, D.; Li, X.; Liu, L.; Yagnik, G. B.; Zhou, F. *J. Phys. Chem. B* **2010**, *114*, 4896–4903.
(23) Erecińska, M.; Silver, I. A. *Respir. Physiol.* **2001**, *128*, 263–276.
(24) Siegel, G. J.; Albers, R. W.; Brady, S.; Price, D. L. *Basic Neurochemistry: Molecular, Cellular, and Medical Aspects*, 7th ed.; Academic Press: London, 2005.
(25) Chattopadhyay, M.; Walter, E. D.; Newell, D. J.; Jackson, P. J.; Aronoff-Spencer, E.; Peisach, J.; Gerfen, G. J.; Bennett, B.; Antholine, W. E.; Millhauser, G. L. *J. Am. Chem. Soc.* **2005**, *127*, 12647–12656.
(26) Walter, E. D.; Chattopadhyay, M.; Millhauser, G. L. *Biochemistry* **2006**, *45*, 13083–13092.
(27) Burns, C. S.; Aronoff-Spencer, E.; Legname, G.; Prusiner, S. B.; Antholine, W. E.; Gerfen, G. J.; Peisach, J.; Millhauser, G. L. *Biochemistry* **2003**, *42*, 6794–6803.
(28) Õsz, K.; Nagy, Z.; Pappalardo, G.; Di Natale, G.; Sanna, D.; Micera, G.; Rizzarelli, E.; Sóvágó, I. *Chem.—Eur. J.* **2007**, *13*, 7129–7143.
(29) Hureau, C.; Charlet, L.; Dorlet, P.; Gonnet, F.; Spadini, L.; Anxolabéhère-Mallart, E.; Girerd, J.-J. *J. Biol. Inorg. Chem.* **2006**, *11*, 735–744.
(30) Davies, P.; Marken, F.; Salter, S.; Brown, D. R. *Biochemistry* **2009**, *48*, 2610–2619.
(31) Stevens, D. J.; Walter, E. D.; Rodriguez, A.; Draper, D.; Davies, P.; Brown, D. R.; Millhauser, G. L. *PLoS Pathog.* **2009**, *5*, 11.
(32) Miura, T.; Sasaki, S.; Toyama, A.; Takeuchi, H. *Biochemistry* **2005**, *44*, 8712–8720.
(33) Ruiz, F. H.; Silva, E.; Inestrosa, N. C. *Biochem. Biophys. Res. Commun.* **2000**, *269*, 491–495.
(34) Aronoff-Spencer, E.; Burns, C. S.; Avdievich, N. I.; Gerfen, G. J.; Peisach, J.; Antholine, W. E.; Ball, H. L.; Cohen, F. E.; Prusiner, S. B.; Millhauser, G. L. *Biochemistry* **2000**, *39*, 13760–13771.
(35) Burns, C. S.; Aronoff-Spencer, E.; Dunham, C. M.; Lario, P.; Avdievich, N. I.; Antholine, W. E.; Olmstead, M. M.; Vrielink, A.; Gerfen, G. J.; Peisach, J.; Scott, W. G.; Millhauser, G. L. *Biochemistry* **2002**, *41*, 3991–4001.
(36) Bonomo, R. P.; Impellizzeri, G.; Pappalardo, G.; Rizzarelli, E.; Tabbì, G. *Chem.—Eur. J.* **2000**, *6*, 4195–4201.
(37) Shiraishi, N.; Ohta, Y.; Nishikimi, M. *Biochem. Biophy. Res. Commun.* **2000**, *267*, 398–402.
(38) Requena, J. R.; Groth, D.; Legname, G.; Stadtman, E. R.; Prusiner, S. B.; Levine, R. L. *Proc. Natl. Acad. Sci. U.S.A.* **2001**, *98*, 7170–7175.
(39) Shearer, J.; Rosenkoetter, K. E.; Callan, P. E.; Pham, C. *Inorg. Chem.* **2011**, *50*, 1173–1175.
(40) Wang, C.; Liu, L.; Zhang, L.; Peng, Y.; Zhou, F. *Biochemistry* **2010**, *49*, 8134–8142.
(41) Peroxidase Electrode Kit, Instruction Manual; http://www.basinc.com/mans/PE-man.pdf (accessed Jul 2010).
(42) Bard, A. J.; Faulkner, L. R. *Electrochemical Methods: Fundamentals and Applications*; John Wiley & Sons, Inc: New York, 2001.
(43) Bonomo, R. P.; Impellizzeri, G.; Pappalardo, G.; Purrello, R.; Rizzarelli, E.; Tabbi, G. *J. Chem. Soc., Dalton Trans.* **1998**, 3851–3857.
(44) Brown, D. R.; Wong, B. S.; Hafiz, F.; Clive, C.; Haswell, S. J.; Jones, I. M. *Biochem. J.* **1999**, *344*, 1–5.
(45) Stańczak, P.; Kozlowski, H. *Biochem. Biophys. Res. Commun.* **2007**, *352*, 198–202.
(46) Yamamoto, N.; Kuwata, K. *J. Biol. Inorg. Chem.* **2009**, *14*, 1209–1218.
(47) Jiang, D.; Men, L.; Wang, J.; Zhang, Y.; Chickenyen, S.; Wang, Y.; Zhou, F. *Biochemistry* **2007**, *46*, 9270–9282.
(48) Nelson, D. L.; Cox, M. M.; Freeman, W. H. *Lehninger Principles of Biochemistry*; W. H. Freeman: New York, 2004.
(49) Conway, B. E. *Electrochemical Data*; Greenwood Press: New York, 1969.
(50) Dryhurst, G.; Kadish, K. M.; Scheller, F.; Renneberg, R. *Biological Electrochemistry*; Academic Press: New York, London, 1982.
(51) Deschamps, P.; Zerrouk, N.; Nicolis, I.; Martens, T.; Curis, E.; Charlot, M. F.; Girerd, J. J.; Prange, T.; Benazeth, S.; Chaumeil, J. C.; Tomas, A. *Inorg. Chim. Acta* **2003**, *353*, 22–34.
(52) Hureau, C.; Mathé, C.; Faller, P.; Mattioli, T. A.; Dorlet, P. *J. Biol. Inorg. Chem.* **2008**, *13*, 1055–1064.
(53) Sayre, L. M. *Science* **1996**, *274*, 1933–1934.
(54) Ivanov, A. I.; Parkinson, J. A.; Cossins, E.; Woodrow, J.; Sadler, P. J. *J. Biol. Inorg. Chem.* **2000**, *5*, 102–109.
(55) Strozyk, D.; Bush, A. I. In *Metal Ions in Life Sciences*; Sigel, A., Sigel, H., Sigel, R. K. O., Eds.; John Wiley & Sons: West Sussex, 2006.
(56) Pall, H. S.; Blake, D. R.; Gutteridge, J. M.; Williams, A. C.; Lunec, J.; Hall, M.; Taylor, A. *Lancet* **1987**, *2*, 238–241.
(57) Zhu, M.; Qin, Z. J.; Hu, D. M.; Munishkina, L. A.; Fink, A. L. *Biochemistry* **2006**, *45*, 8135–8142.
(58) Varadarajan, S.; Yatin, S.; Aksenova, M.; Butterfield, D. A. *J. Struct. Biol.* **2000**, *130*, 184–208.
(59) Smith, M. A.; Joseph, J. A.; Perry, G. *Ann. N.Y. Acad. Sci.* **2000**, *924*, 35–38.
(60) Pauly, P. C.; Harris, D. A. *J. Biol. Chem.* **1998**, *273*, 33107–33110.
(61) Jovic, M.; Sharma, M.; Rahajeng, J.; Caplan, S. *Histol. Histopath.* **2010**, *25*, 99–112.
(62) Luzio, J. P.; Rous, B. A.; Bright, N. A.; Pryor, P. R.; Mullock, B. M.; Piper, R. C. *J. Cell Sci.* **2000**, *113*, 1515–1524.
(63) Brown, D. R.; Schmidt, B.; Kretzschmar, H. A. *J. Neurochem.* **1998**, *70*, 1686–1693.
(64) Chen, B. T.; Avshalumov, M. V.; Rice, M. E. *J. Neurophysiol.* **2001**, *85*, 2468–2476.
(65) Nishimura, T.; Sakudo, A.; Nakamura, I.; Lee, D. C.; Taniuchi, Y.; Saeki, K.; Matsumoto, Y.; Ogawa, M.; Sakaguchi, S.; Itohara, S.; Onodera, T. *Biochem. Biophys. Res. Commun.* **2004**, *323*, 218–222.
(66) Cohen, G. *Ann. N.Y. Acad. Sci.* **1994**, *738*, 8–15.
(67) Forman, H. J.; Maiorino, M.; F., U. *Biochemistry* **2010**, *49*, 935–842.
(68) Veal, E. A.; Day, A. M.; Morgan, B. A. *Mol. Cell* **2007**, *26*, 1–14.
(69) Rhee, S. G. *Science* **2006**, *312*, 1882–1883.
(70) Stone, J. R.; Yang, S. *Antioxid. Redox Signaling* **2006**, *8*, 243–270.
(71) Herms, J.; Tings, T.; Gall, S.; Madlung, A.; Giese, A.; Siebert, H.; Schurmann, P.; Windl, O.; Brose, N.; Kretzschmar, H. *J. Neurosci.* **1999**, *19*, 8866–8875.
(72) Mouillet-Richard, S.; Ermonval, M.; Chebassier, C.; Laplanche, J. L.; Lehmann, S.; Launay, J. M.; Kellermann, O. *Science* **2000**, *289*, 1925–1928.